Highlights on Spanish Astrophysics X, Proceedings of the XIII Scientific Meeting of the Spanish Astronomical Society held on July 16 – 20, 2018, in Salamanca, Spain. B. Montesinos, A. Asensio Ramos, F. Buitrago, R. Schödel, E. Villaver, S. Pérez-Hoyos, I. Ordóñez-Etxeberria (eds.), 2019

Signatures of primordial black holes as seeds of supermassive black holes.

José Luis Bernal[1,2], Alvise Raccanelli[1,3], Licia Verde[1,4] and Joseph Silk[5,6,7]

[1] Institut de Ciències del Cosmos (ICCUB), Universitat de Barcelona (IEEC-UB), Martí Franquès 1, E08028 Barcelona, Spain
[2] Dept. de Física Quàntica i Astrofísica, Universitat de Barcelona, Martí i Franquès 1, E08028 Barcelona, Spain
[3] Theoretical Physics Department, CERN, 1 Esplanade des Particules, CH-1211 Geneva 23, Switzerland
[4] ICREA, Pg. Lluís Companys 23, 08010 Barcelona, Spain
[5] Department of Physics and Astronomy, Johns Hopkins University, 3400 N. Charles St., Baltimore, MD 21218
[6] Institut d'Astrophysique de Paris, UMR 7095, CNRS, UPMC Univ. Paris VI, 98 bis Boulevard Arago, 75014 Paris, France
[7] BIPAC, Department of Physics, University of Oxford, Keble Road, Oxford OX1 3RH, UK

Abstract

It is broadly accepted that Supermassive Black Holes (SMBHs) are located in the centers of most massive galaxies, although there is still no convincing scenario for the origin of their massive seeds. It has been suggested that primordial black holes (PBHs) of masses $\gtrsim 10^2\ M_\odot$ may provide such seeds, which would grow to become SMBHs. We suggest an observational test to constrain this hypothesis: gas accretion around PBHs during the cosmic dark ages powers the emission of high energy photons which would modify the spin temperature as measured by 21cm Intensity Mapping (IM) observations. We model and compute their contribution to the standard sky-averaged signal and power spectrum of 21cm IM, accounting for its substructure and angular dependence for the first time. While SKA could provide a detection, only a more ambitious experiment would provide accurate measurements.

1 Introduction

We know that Supermassive Black Holes (SMBHs) inhabit the centers of most galaxies: observations of quasars at $z \sim 6-7$ indicate that, even at these early times, there were SMBHs with masses of several $10^9 M_\odot$ (e.g., [2]). The existence of a population of intermediate mass

black holes of masses around $10^2 - 10^6 M_\odot$ at $z \sim 20 - 15$ would suffice to seed them. However, the origin and formation mechanism of the massive seeds are still uncertain. There are two main scenarios proposed to explain their origin.

According to the first hypothesis, the seeds of SMBHs are remnants of Population III stars, formed with masses of tens of solar masses at $z \gtrsim 20$, which grow due to gas accretion and mergers. However, in order to reach masses such as those observed at $z \sim 6 - 7$, supercritical accretion over extended periods of time is needed [7]. However, cosmic X-ray background observations impose constraints on the growth of SMBHs, constraining the abundance of quasars with supercritical accretion and miniquasars at high redshift [9].

On the other hand, SMBH seeds might also be formed due to the collapse of gas clouds which do not fragment or form ordinary stars, but directly form a massive black hole ($M \sim 10^5 - 10^6 M_\odot$) at lower redshifts ($z \lesssim 15$) [6]. This kind of seed is called a Direct Collapse Black Hole (DCBH). Moreover, DCBHs are a good candidate for explaining the large-scale power spectrum of the Near Infrared Background and its cross correlation with the cosmic X-ray background [10], and there are candidates of possible detections. Nonetheless, the exact conditions and the probability of obtaining DCBHs are still uncertain; recent theoretical studies suggest that this mechanism might explain the abundance of the most luminous quasars at $z \sim 6 - 7$, but not the general population of SMBHs.

In summary, neither of these two scenarios individually provide an entirely convincing explanation for the origin of the seeds of SMBHs. However, Primordial Black Holes (PBHs) might be the seeds which will grow to become SMBHs. The mass range required for PBHs to be the seeds of SMBHs without requiring supercritical accretion is $\gtrsim 10^2 M_\odot$. In this mass range, the PBH abundance, $f_{\rm PBH} = \Omega_{\rm PBH}/\Omega_{\rm CDM}$, is strongly constrained by e.g., CMB observations [1, 4]. However, if PBHs of these masses are only required to be the seeds of SMBHs and not a substantial part of the dark matter, $f_{\rm PBH} \sim 10^{-8} - 10^{-6}$ (which satisfies all observational constraints) is enough.

In this work, we focus on the imprints of PBHs as seeds of SMBHs on 21 cm Intensity Mapping (IM). Observations of spin temperature maps in the dark ages provide a direct window into the matter density fluctuations free of complications such as galaxy bias and most astrophysical processes. Therefore, in order to avoid astrophysical uncertainties, we concentrate on the dark ages ($z \gtrsim 30$). Besides, if massive seeds are to be found in these redshifts, they must be primordial. We model the signature of massive PBHs, with abundances required to explain the current SMBH population in the 21 cm IM signal. We compute 2-point statistics of the fluctuations accounting explicitly for the brightness temperature (T_{21}) profiles around the PBHs in a comprehensive way, for the first time. The work and results reported on this Proceeding are collected more complete and with further discussion in [5].

2 Effects of PBHs on the 21cm IM signal

The presence of PBHs affects the gas spin temperature: the PBH accretion triggers the emission of high-energy photons which heat and ionize the gas around. We assume that all processes are in equilibrium, given that their timescales are much smaller than the Hubble

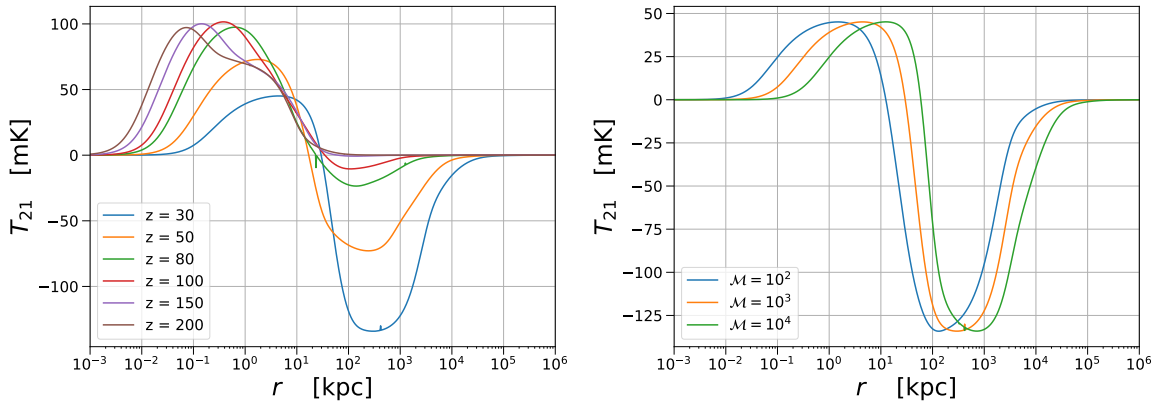

Figure 1: Differential brightness temperature profile for a PBH with $\mathcal{M} = 100$ at various redshifts (left) and for a PBH with various values of $\mathcal{M}$ at $z = 30$ (right).

timescale. The steady-state approximation is very precise for masses $M \lesssim 3 \times 10^4 M_\odot$ [8], so we limit our exploration to $M \leq 10^4 M_\odot$. Given the slow growth of the PBHs at $z \gtrsim 30$, we assume that the PBH mass at different redshifts is the same. Finally, we consider for simplicity that all PBHs have the same mass. This is an unrealistic scenario, but constraints for monochromatic mass distributions can be translated to any extended mass distribution using e.g., the methods proposed in [3].

We assume that gas accretion around the PBH powers a spherically symmetric X-ray emission, $F(E) = \mathcal{A}(M\lambda)\ E^{-1}\mathrm{s}^{-1}$, where $\mathcal{A}$ is a normalization factor chosen to have a luminosity $L = \lambda L_{\mathrm{Edd}}$, where λ is the Eddington ratio and L_{Edd} is the Eddington luminosity. Relevant quantities, as the neutral fraction, x_H, or T_{21}, only depend on the redshift and the intensity of the emission. Therefore, in order to illustrate how these quantities depend on both λ and M, we will show them in terms of $\mathcal{M} = M\lambda$.

The ionized and heated region around the PBH changes with redshift and $\mathcal{M}$. With increasing redshift, the hydrogen density increases; in a given volume at fixed photon flux, there are more atoms to ionize, hence the size of the ionized region decreases. On the other hand, for larger $\mathcal{M}$, as the PBH emission is more intense, the ionized region becomes larger. In the inner regions, the heating due to the emission of the PBH is coupled only to the neutral hydrogen, but, as the number of photons decays exponentially with the distance, this heating is more efficient close to the PBH. At intermediate distances, PBH heating loses efficiency and T_k drops even below the CMB temperature.

Due to the modified neutral fraction and kinetic temperature of the gas, a bubble with spin temperature, hence T_{21}, different from the background value is formed around the PBH. The $T_{21}(r)$ profile shown in 1 can be explained as follows. In the inner part, $T_{21} = 0$ because all of the gas is ionized. The region with $T_{21} > 0$ corresponds to the region where $T_k > T_{\mathrm{CMB}}$ and x_H starts to grow; then, where T_k drops because the PBH heating is less efficient, T_{21} drops to negative values. Finally, T_{21} rises again due to the collisional and Lyman-α coupling of the photons to the source with the gas becomes totally inefficient. Given that we consider

the isolated PBH signal, at these distances, $T_{21} = 0$.

3 PBH contribution to the power spectrum

We use the halo model to characterize the total T_{21} angular power spectrum during the dark ages in the presence of PBHs: $C_\ell^{\rm PBH} = C_\ell^{\rm PBH(1h)} + C_\ell^{\rm PBH(2h)}$. We compute the observed fluctuations on T_{21} produced by a population of PBHs with number density $n_{\rm PBH}$. As the standard contribution in the linear regime without the PBHs comes from a continuum where there are no haloes, we consider that the one-halo term of the standard contribution vanishes. Therefore, the total angular power spectrum is the sum of:

$$C_\ell^{\rm PBH(1h)} = \frac{2}{\pi} n_{\rm PBH} \int_0^\infty dk k^2 \left(\mathcal{T}_\ell^{\rm PBH}\right)^2; \; C_\ell^{\rm PBH(2h)} = \frac{2}{\pi} \int_0^\infty dk k^2 \left(\mathcal{T}_\ell + n_{\rm PBH} b \mathcal{T}_\ell^{\rm PBH}\right)^2 P_m(k), \tag{1}$$

where $\mathcal{T}_\ell$ and $\mathcal{T}_\ell^{\rm PBH}$ are the transfer function for the 21 cm IM fluctuations due to the standard contribution and the PBHs, respectively, $P_m(k)$ is the matter power spectrum, b is a scale-independent bias, and we assume that PBHs are completely correlated with the dark matter distribution. Given that the formation of a PBH is a rare event and PBHs spatial distribution is discrete, there is a Poissonian fluctuation in the number density of PBHs. Therefore, in addition to the standard matter power spectrum, there is an extra contribution, $P_{\rm Poisson}(z) = \frac{9}{4}(1+z_{\rm eq})^2 D^2(z) \frac{f_{\rm PBH}^2}{n_{\rm PBH}}$, where $D(z)$ is the growth factor.

It is easy to notice that the PBH contribution depends only on two quantities besides the redshift: $n_{\rm PBH}$ and $\mathcal{T}_\ell^{\rm PBH}$. Therefore, although we do consider three parameters regarding PBHs (M, λ and $\Omega_{\rm PBH}$), the relevant quantities are combinations of them: $\mathcal{M} = M\lambda$ and $n_{\rm PBH} \propto \Omega_{\rm PBH}/M$. Essentially, varying $\mathcal{M}$ shifts the features related with PBHs to different multipole ranges (via $\mathcal{T}_\ell^{\rm PBH}$). The latter is a rescaling of the amplitude of such contributions. These two effects are relevant to determine at which scale the PBH contribution starts to dominate. We show how the total angular power spectrum changes with respect to the PBH parameters and the redshift in Figure 2. As can be seen, the PBH-induced deviation from the standard signal decreases with redshift because the size of the bubble also does it (see Figure 1), so the scale at which the deviation is appreciable increases.

4 Conclusions

The origin and formation mechanism of SMBHs remains largely unknown. There are three candidates to be the seeds of SMBHs: remnants of Population III stars, DCBHs or PBHs. In this work, we address the observational signatures that intermediate mass PBHs would have on 21 cm IM during the dark ages. We model this signal starting from the characterization of the radial profiles of T_{21} around a single PBH to compute the contribution to the angular power spectrum, using the halo model. This is the first time that the signature of PBHs

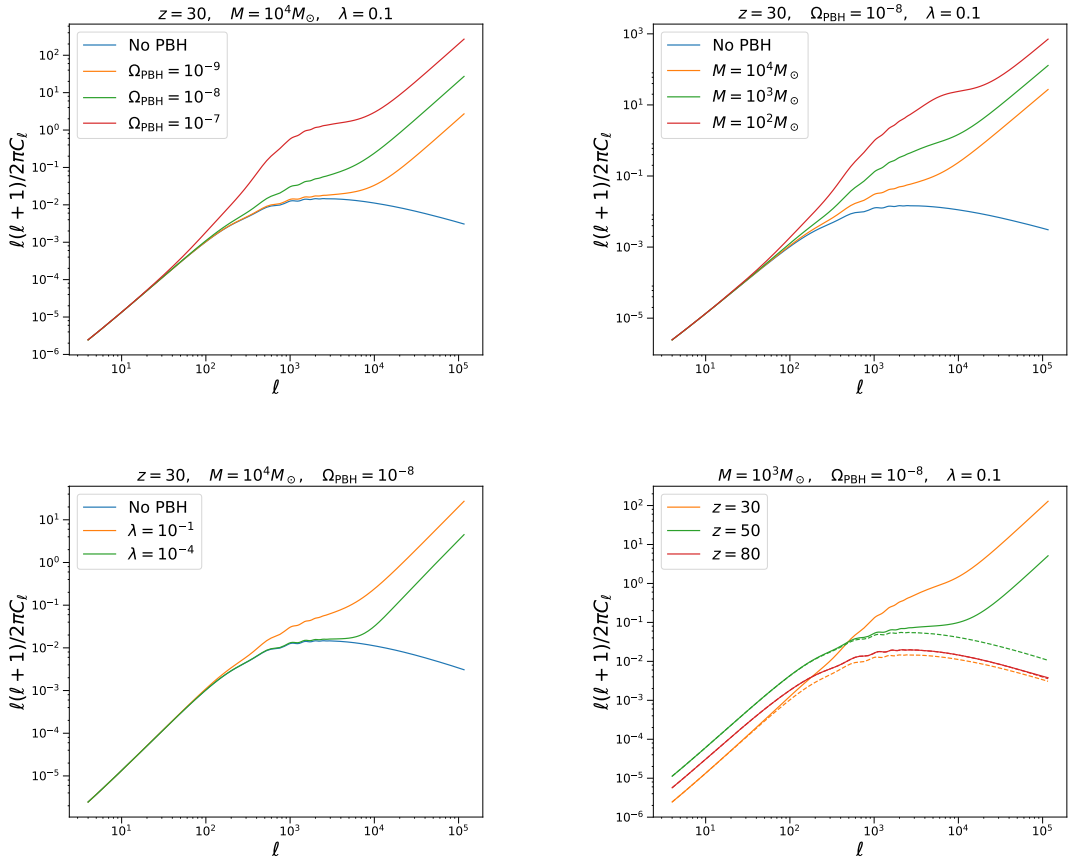

Figure 2: Angular power spectrum of the total signal in 21 cm IM at $z = 30$ varying the the density parameter of PBH (top left), the mass (top right) and the Eddington ratio (bottom left), and varying redshift for $M = 10^3 M_\odot$, $\Omega_{\rm PBH} = 10^{-8}$, $\lambda = 0.1$ (bottom right).

accounting for its full scale dependence is modeled in the 21 cm IM power spectrum. We consider several configurations of the PBH parameters, since they are largely unconstrained.

The presence of PBHs increases the amplitude of the 21 cm IM angular power spectrum for $\ell \gtrsim 10^2 - 10^3$, which decays with redshift. We forecast the detectability of the PBH contribution and the potential to measure the PBH parameters by future experiments, ranging from SKA to more ambitious futuristic ground experiment, as well as radio array in the far side of the Moon. Given that the atmosphere is opaque for frequencies $\lesssim 45$ MHz, a ground experiment will not be able to observe much further than $z \approx 30$; however, with the lunar radio arrays, tomography for $30 \lesssim z \lesssim 200$ is possible. The PBH signal will be barely detected by SKA, since only for extreme cases in which $n_{\rm PBH}$ is very large, the signal-to-noise ratio, S/N, for $\Omega_{\rm PBH}$ and λ is larger than unity. As the amplitude of the power spectrum increases greatly at small scales, being able to resolve very small scales (i.e., large interferometer baseline, which implies large $\ell_{\rm cover}$) will be key to detect the PBH signal and constrain

the parameters. On the other hand, the contribution of PBHs to the power spectrum decays with redshift (see Figure 2), hence the S/N between the case with PBHs and the standard one decreases fast with redshift. As tomography does not add much information, $\ell_{\rm cover}$ has more impact in the final S/N

To summarize, although a detection of the PBH contribution in the dark ages might be achieved by SKA, in order to measure $\Omega_{\rm PBH}$ and λ accurately, a more ambitious experiment with a larger baseline is needed. Such measurements will be more precise if tomography is possible, for which experiments such as a lunar radio array are needed.

The advent of new experiments and corresponding observations will shed light on how SMBHs reached such huge masses and on the nature of the massive seeds needed to explain their existence. It is also possible that the three kinds of seeds discussed above coexist and give different signatures. We eagerly await observations that will open the window toward higher redshifts and will give us the opportunity to improve our understanding of some of the most extreme structures in the Universe.

Acknowledgments

Funding for this work was partially provided by the Spanish MINECO under projects AYA2014-58747-P AEI/FEDER UE and MDM-2014-0369 of ICCUB (Unidad de Excelencia Maria de Maeztu). JLB is supported by the Spanish MINECO under grant BES-2015-071307, co-funded by the ESF and thanks the Royal Observatory of Edinburgh for hospitality. AR has received funding from the People Programme (Marie Curie Actions) of the European Union H2020 Programme under REA grant agreement number 706896 (COSMOFLAGS). LV acknowledges support of European Union's Horizon 2020 research and innovation programme ERC (BePreSySe, grant agreement 725327).

References

[1] Ali-Haimoud, Y. & Kamionkowski, M., 2017, PRD, 95, 043534

[2] Bañados, E. et al. 2018, Nature, 553, 473

[3] Bellomo, N., Bernal, J. L., Raccanelli, A., Verde, L., 2018, JCAP01(2018)004

[4] Bernal, J. L., Bellomo, N., Raccanelli, A., Verde, L., 2017, JCAP10(2017)052

[5] Bernal, J. L., Raccanelli, A., Verde, L., Silk, J., 2018, JCAP05(2018)017

[6] Bromm, V. & Loeb, A., 2003, ApJ 596, 34

[7] Inayoshi, K., Haiman, Z., Ostriker, J. P., 2016, MNRAS, 459, 3738

[8] Ricotti, M., 2007, ApJ, 662, 53

[9] Salvaterra, R., Haardt, F., Volonteri, M., Moretti, A., 2012, A&A, 545, L6

[10] Yue, B., Ferrara, A., Salvaterra, R., Xu, Y., Chen, X., 2013, MNRAS 433, 1556